

**Electronic Supplementary Information**

**Two-dimensional porous porphyrin materials composed of  
robust tin(IV)-porphyrin linkages for photocatalytic  
wastewater remediation**

Nirmal Kumar Shee and Hee-Joon Kim\*

*Department of Chemistry and Bioscience, Kumoh National Institute of Technology  
Gumi 39177, Republic of Korea*

## List of contents:

1. Synthesis of *trans*-dihydroxo[5,10,15,20-tetraphenylporphyrinato]tin(IV) (SnP)
2. Synthesis of [5,10,15,20-tetrakis(4-carboxyphenyl)porphyrin] (H<sub>2</sub>TCPP)
3. Synthesis of [5,10,15,20-tetrakis(4-carboxyphenyl)porphyrinato]zinc(II) (ZnTCPP)

**Fig. S1** TGA thermogram of **SnP-H<sub>2</sub>TCPP** and **SnP-ZnTCPP**.

**Fig. S2** Adsorption and desorption isotherms of N<sub>2</sub> for **SnP-H<sub>2</sub>TCPP** at 77 K.

**Fig. S3** Adsorption and desorption isotherms of N<sub>2</sub> for **SnP-ZnTCPP** at 77 K.

**Fig. S4** FE-SEM images of (a) SnP, (b) H<sub>2</sub>TCPP, and (c) ZnTCPP.

**Fig. S5** Energy dispersive X-ray spectroscopy (EDS) for **SnP-H<sub>2</sub>TCPP**.

**Fig. S6** Energy dispersive X-ray spectroscopy (EDS) for **SnP-ZnTCPP**.

**Fig. S7** MB dye adsorption tests for **SnP-H<sub>2</sub>TCPP (1)** and **SnP-ZnTCPP**.

**Fig. S8** Time dependent absorption spectra of MB dye in the presence of **SnP-ZnTCPP** under visible light irradiation.

**Fig. S9** Kinetics of the photocatalytic degradation of MB under visible light irradiation.

**Fig. S10** Absorption spectra of TC in the presence of **SnP-ZnTCPP** under visible light irradiation.

**Fig. S11** Kinetics of the photocatalytic degradation of TC under visible light irradiation.

**Fig. S12** Recyclability of the photocatalyst **SnP-H<sub>2</sub>TCPP** towards the degradation of MB dye.

**Fig. S13** FE-SEM images of **SnP-H<sub>2</sub>TCPP** (before and after the degradation of MB).

**Fig. S14** FT-IR spectra of **SnP-H<sub>2</sub>TCPP** (before and after the degradation of MB).

**Fig. S15** PXRD patterns of **SnP-H<sub>2</sub>TCPP** (before and after the degradation of MB).

**Fig. S16** Effect of temperature on the photocatalytic degradation of MB dye in the presence of **SnP-ZnTCPP**.

**Fig. S17** Effect of pH on the degradation of MB dye solution in the presence of **SnP-ZnTCPP**.

**Fig. S18** Effect of dye concentration on the photocatalytic degradation of MB dye in the presence of **SnP-ZnTCPP**.

**Fig. S19** Effect of wavelength on the photocatalytic degradation of MB dye in the presence of **SnP-H<sub>2</sub>TCPP**.

**Fig. S20** Positive ion mode ESI-MS spectrum for the MB dye degradation reaction by **SnP-H<sub>2</sub>TCPP** after 60 min of visible light irradiation.

**Fig. S21** Possible intermediates formed during MB dye degradation in the presence of **SnP-H<sub>2</sub>TCPP** after 60 min of visible light irradiation.

**Fig. S22** Band gap energy of SnP, H<sub>2</sub>TCPP, ZnTCPP, **SnP-H<sub>2</sub>TCPP**, and **SnP-ZnTCPP**, calculated from Tauc Plots using UV-vis absorption spectral data.

**Fig. S23** Photocurrent responses for **SnP-H<sub>2</sub>TCPP** and **SnP-ZnTCPP** under visible light.

**Fig. S24** EIS Nyquist plots for **SnP-H<sub>2</sub>TCPP** and **SnP-ZnTCPP** under visible light.

**Fig. S25** Visible light MB dye degradation activity of **SnP-ZnTCPP** in the presence of various scavengers.

## 1. Synthesis of *trans*-dihydroxo[5,10,15,20-tetraphenylporphyrinato]tin(IV) (SnP)

### 1.1 Synthesis of 5,10,15,20-tetraphenylporphyrin ( $H_2TPP$ )

Freshly distilled pyrrole (2.7 g, 2.8 mL, 40 mmol) and benzaldehyde (4.3 g, 4.1 mL, 40 mmol) were dissolved in propionic acid (400 mL) and refluxed for 2 h. After that, the reaction mixture was kept overnight at 10 °C. The crude product was then filtered and washed with MeOH, followed by water. The resulting purple solid was then dried under reduced pressure. Yield: 1.48 g (24%).  $^1H$  NMR (400 MHz,  $CDCl_3$ ,  $\delta$  in ppm): 8.83 (s, 8H,  $\beta$ -pyrrole), 8.20 (d,  $J = 7.6$  Hz, 8H, *meso*-O-phenyl), 7.70-7.78 (m, 12H, H3, H4, H5-phenyl), -2.81 (s, 2H, NH).

### 1.2 Synthesis of *trans*-dichloro[5,10,15,20-tetraphenylporphyrinato]tin(IV) ( $SnCl_2TPP$ )

$H_2TPP$  (470 mg, 0.77 mmol) and  $SnCl_2 \cdot 2H_2O$  (390 mg, 1.72 mmol) were mixed with pyridine (100 mL) and refluxed for 12 h. After that, pyridine was removed under reduced pressure. The solid product was dissolved in dichloromethane (100 mL) and filtered through a Celite pad. After that, *n*-hexane (100 mL) was added to the above solution with constant stirring. The resulting solid was then filtered, dried in an oven, and then recrystallized from 100 mL of  $CH_2Cl_2/n$ -hexane (1:1). Yield: 0.52 g (85%).  $^1H$  NMR (400 MHz,  $CDCl_3$ ,  $\delta$  in ppm): 9.19 (s, 8H,  $\beta$ -pyrrole), 8.32 (d,  $J = 7.6$  Hz, 8H, *meso*-O-phenyl), 7.82-7.88 (m, 12H, H3, H4, H5-phenyl).

### 1.3 Synthesis of *trans*-dihydroxo[5,10,15,20-tetraphenylporphyrinato]tin(IV) (SnP)

$SnCl_2TPP$  (0.5 g, 0.62 mmol) dissolved in THF (40 mL) was mixed into a solution of  $K_2CO_3$  (0.415 g, 3.0 mmol) in  $H_2O$  (10 mL) and refluxed with constant stirring. After 6 h, the THF was removed under reduced pressure. The resulting purple precipitate was filtered and washed with excess hot water, then dried in air. The crude solid was recrystallized from 100 mL of  $CH_2Cl_2/n$ -hexane (1:1). Yield: 0.38 g (80%). mp > 300 °C.  $^1H$  NMR (400 MHz,  $CDCl_3$ ,  $\delta$  in ppm): 9.11 (s, 8H,  $\beta$ -pyrrole), 8.33 (d,  $J = 7.6$  Hz, 8H, *meso*-O-phenyl), 7.78-7.84 (m, 12H, H3, H4, H5-phenyl), -7.48 (s, 2H, Sn-OH). UV-visible ( $CHCl_3$ ):  $\lambda_{nm}$  (log  $\epsilon$ ), 424 (5.57), 518 (3.12), 558 (4.32), 598 (3.96). Emission ( $CHCl_3$ ,  $\lambda_{ex} = 550$  nm): 623 nm and 675 nm.

## 2. Synthesis of [5,10,15,20-tetrakis(4-carboxyphenyl)porphyrin] (H<sub>2</sub>T CPP)

Pyrrole (2.68 g, 2.8 mL, 40 mmol) and 4-formylbenzoic acid (6.0 g, 40 mmol) were mixed in propionic acid (400 mL) and refluxed. After 2 h, the reaction mixture was cooled to 10 °C and maintained at that temperature overnight. The solid residues were then filtered, washed with cold MeOH, and then dried in air. After that, the crude product was dissolved in 0.1 N NaOH, and the insoluble impurities were removed by filtration; the remaining filtrate was then neutralized with 0.1 N HCl. Finally, the purple precipitate was filtered and dried. Yield: 2.05 g (26%). Melting point > 300 °C. <sup>1</sup>H NMR (400 MHz, DMSO-*d*<sub>6</sub>, δ in ppm): 13.22 (s, 4H, CO<sub>2</sub>H), 8.86 (s, 8H, β-pyrrole), 8.22 (d, *J* = 7.6 Hz, 8H, *meso*-*O*-phenyl), 7.85 (d, *J* = 7.6 Hz, 8H, H<sub>3</sub>, 5-phenyl), -2.94 (s, 2H, NH). UV-visible (THF): λ<sub>nm</sub> (log ε), 418 (5.62), 513 (4.24), 548 (3.89), 591 (3.69), and 646 (3.57). Photoluminescence (THF, λ<sub>ex</sub> = 550 nm): 672 nm and 733 nm.

## 3. Synthesis of [5,10,15,20-tetrakis(4-carboxyphenyl)porphyrinato]zinc(II) (ZnT CPP)

A mixture of H<sub>2</sub>T CPP (1.0 g, 1.26 mmol) and Zn(OAc)<sub>2</sub>·2H<sub>2</sub>O (1.1 g, 5.04 mmol) were added into DMF (140 mL) and heated at 100 °C. After 2 h, the solution was cooled to 10 °C and maintained at that temperature overnight. The solid residue was filtered and washed with DMF, followed by deionized water. The crude product was then dissolved in 0.1 N NaOH solution, and the insoluble solid impurities were removed by filtration. The product was then re-precipitated by neutralizing the filtrate with 0.1 N HCl. Finally, the purple precipitate was filtered and dried. Yield 0.97 g (90%); melting point > 300 °C. <sup>1</sup>H NMR (400 MHz, DMSO-*d*<sub>6</sub>, δ in ppm): 12.86 (s, 4H, -CO<sub>2</sub>H), 8.79 (s, 4H, β-pyrrole), 8.36 (d, *J* = 8.8 Hz, 8H, *meso*-*O*-phenyl), 8.30 (d, *J* = 7.2 Hz, 8H, H<sub>3</sub>, 5-phenyl). UV-visible (H<sub>2</sub>O): λ<sub>nm</sub> (log ε), 426 (5.41), 562 (3.88), and 601 (3.52). Photoluminescence (H<sub>2</sub>O, λ<sub>ex</sub> = 550 nm): 629 nm, and 677 nm.

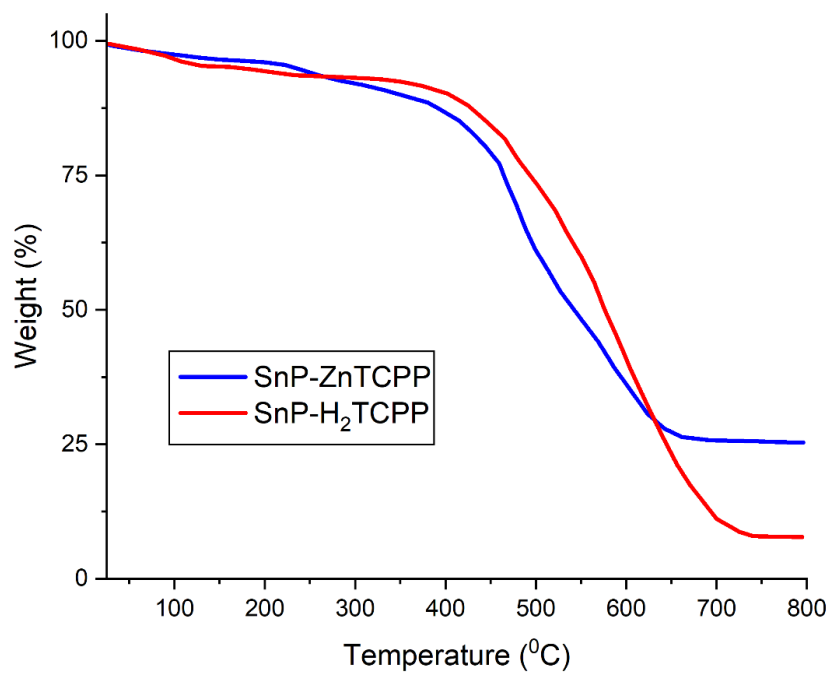


**Fig. S1** TGA thermogram of **SnP-H<sub>2</sub>TCPP** and **SnP-ZnTCPP**.

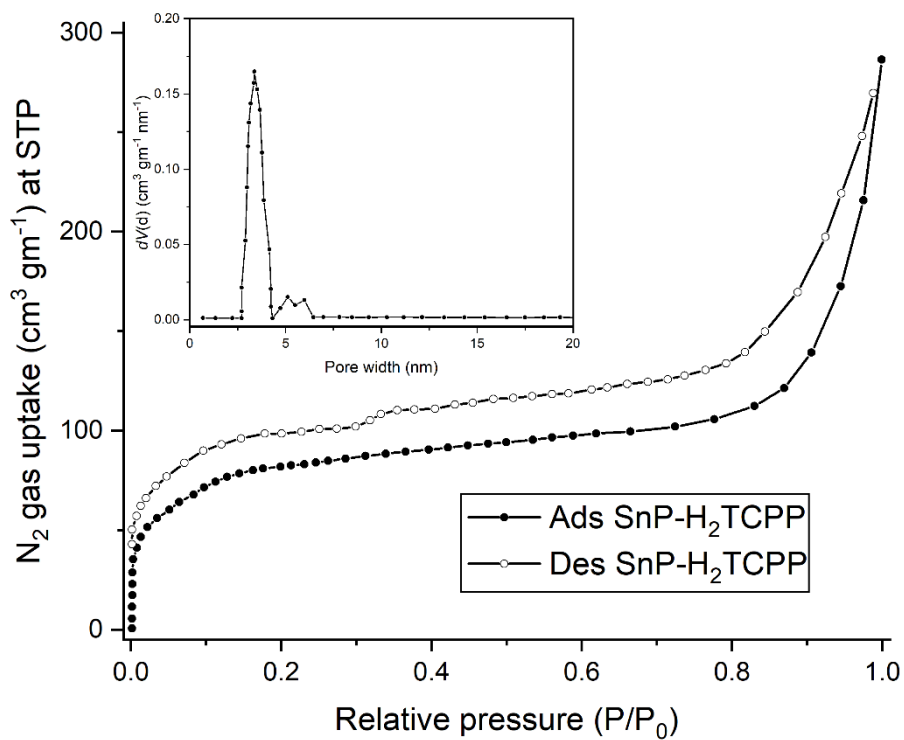


**Fig. S2** Adsorption and desorption isotherms of N<sub>2</sub> for **SnP-H<sub>2</sub>TCPP**.

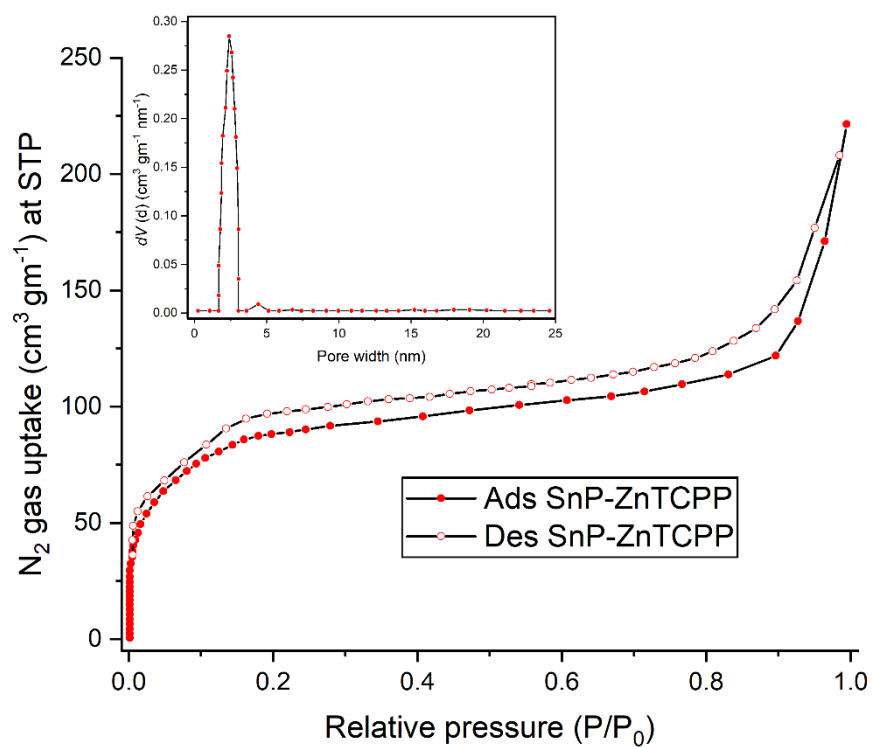


**Fig. S3** Adsorption and desorption isotherms of N<sub>2</sub> for SnP-ZnTCPP at 77 K.

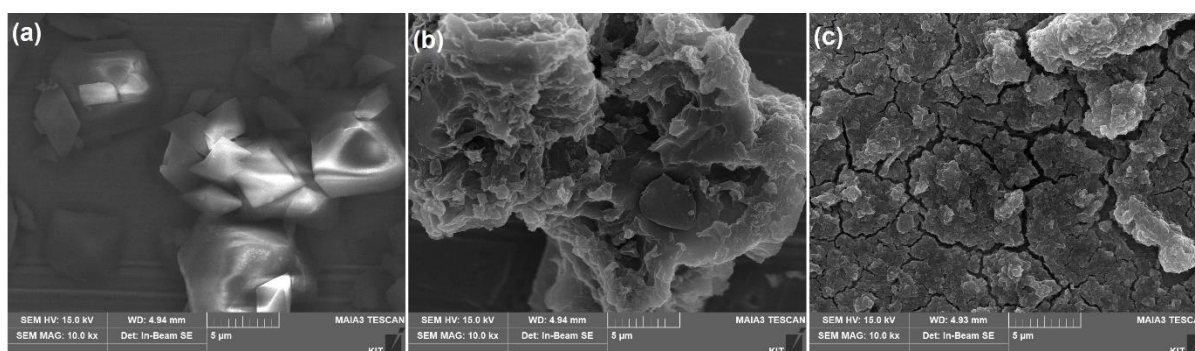
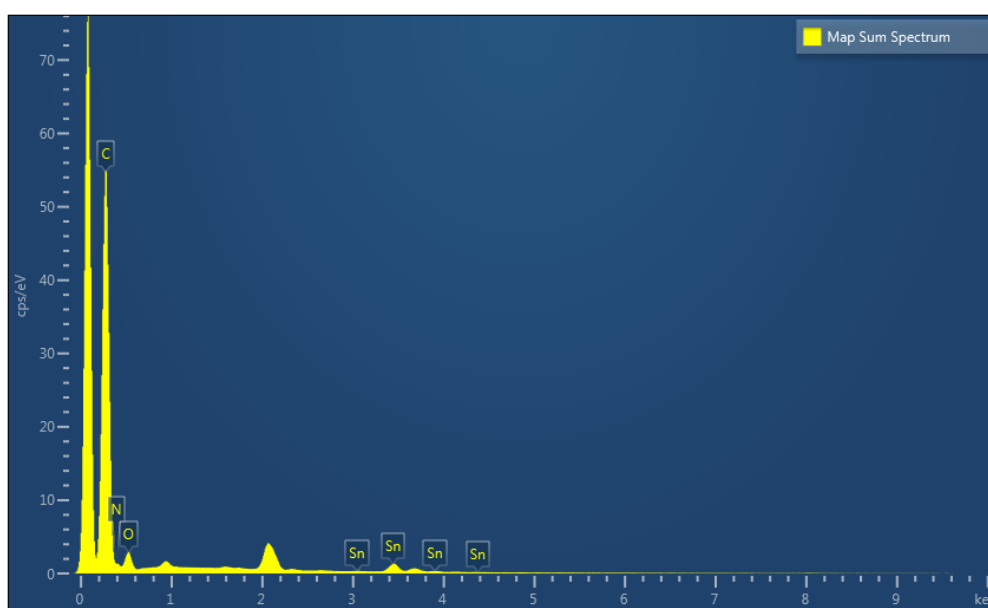
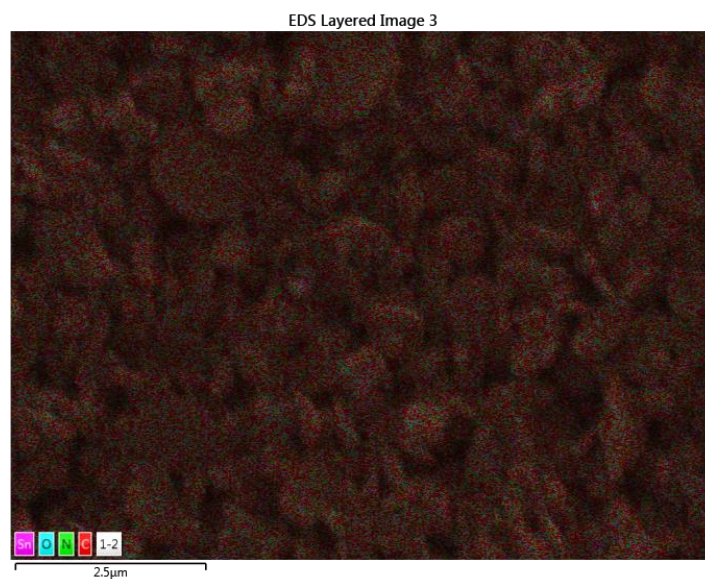


**Fig. S4** FE-SEM images of (a) SnP, (b) H<sub>2</sub>TCPP, and (c) ZnTCPP.

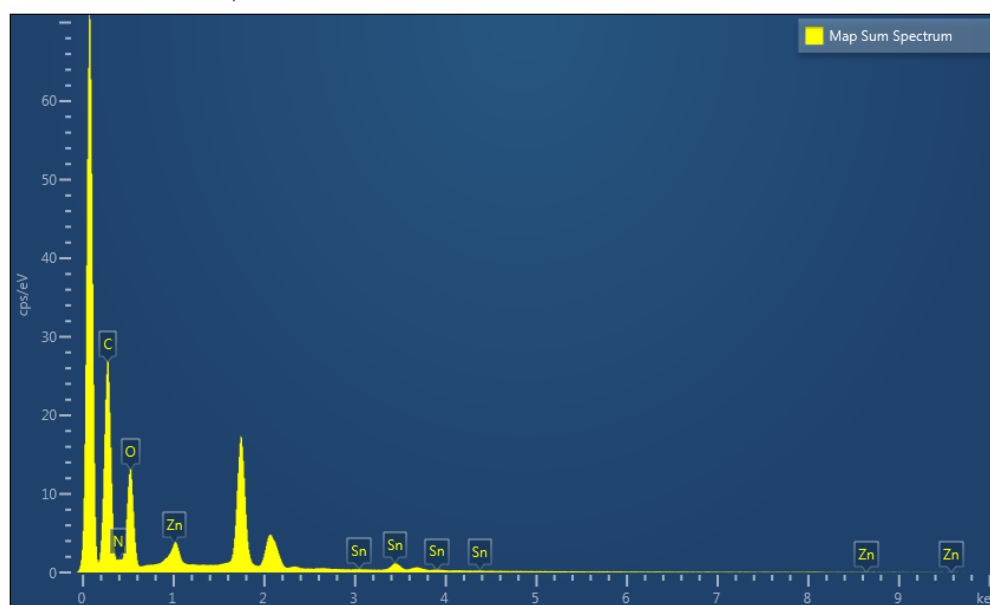


Element	Wt%	Atomic %
C	73.11	84.44
N	7.74	7.66
O	7.55	6.54
Sn	11.60	1.36
Total:	100.00	100.00

**Fig. S5** Energy dispersive X-ray spectroscopy (EDS) for **SnP-H<sub>2</sub>TCPP**.



EDS Layered Image 8



Element	Wt%	Atomic %
C	71.23	83.80
N	7.42	7.48
O	7.72	6.81
Zn	2.97	0.64
Sn	10.66	1.27
Total:	100.00	100.00

Fig. S6 Energy dispersive X-ray spectroscopy (EDS) for SnP-ZnTCPP.

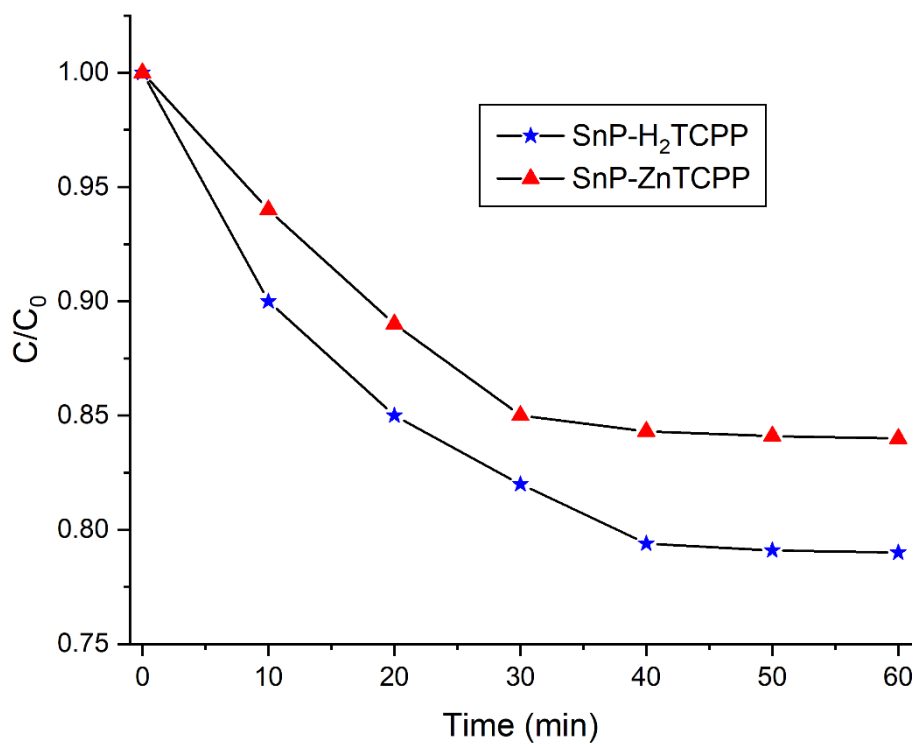


**Fig. S7** MB dye adsorption tests for **SnP-H<sub>2</sub>TCPP** and **SnP-ZnTCPP**.

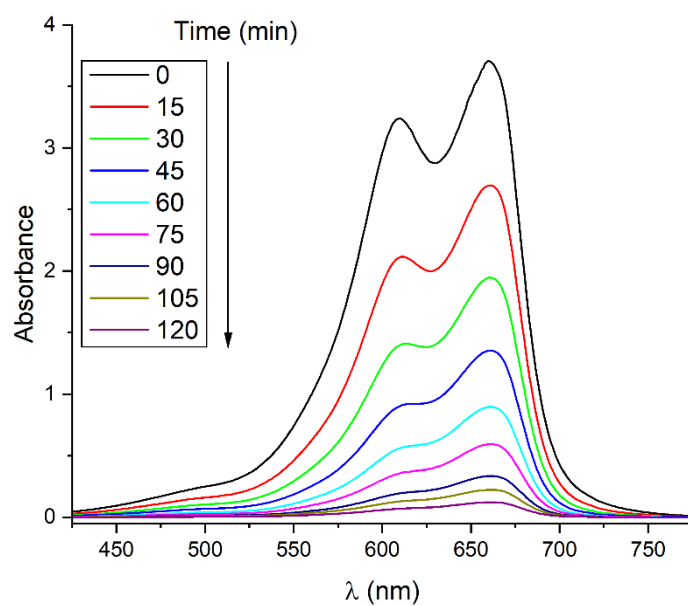


**Fig. S8** Time dependent absorption spectra of MB dye in the presence of **SnP-ZnTCPP** under visible light irradiation.

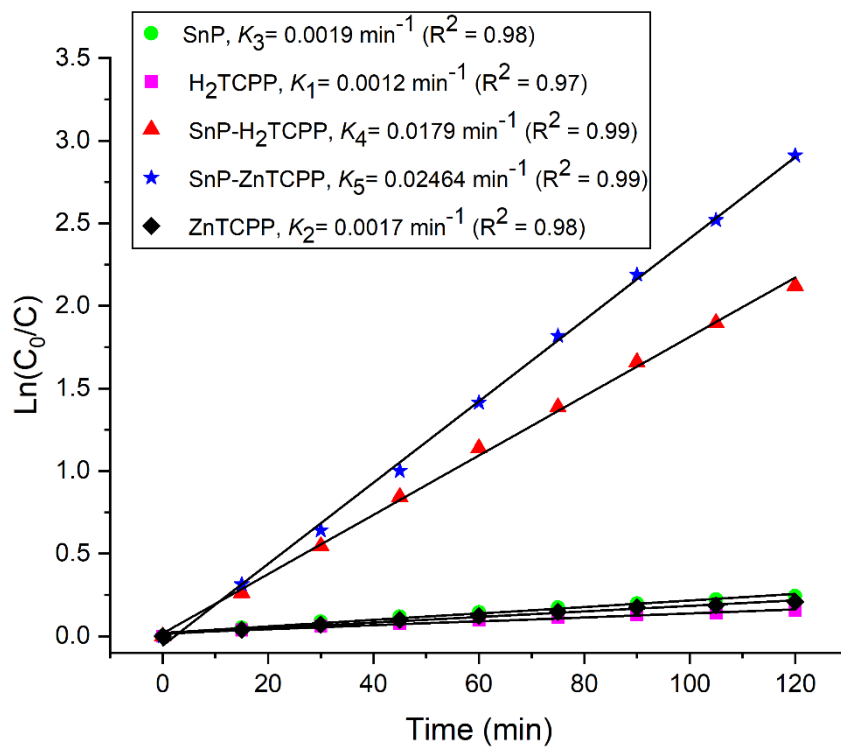


**Fig. S9** Kinetics of the photocatalytic degradation of MB under visible light irradiation.

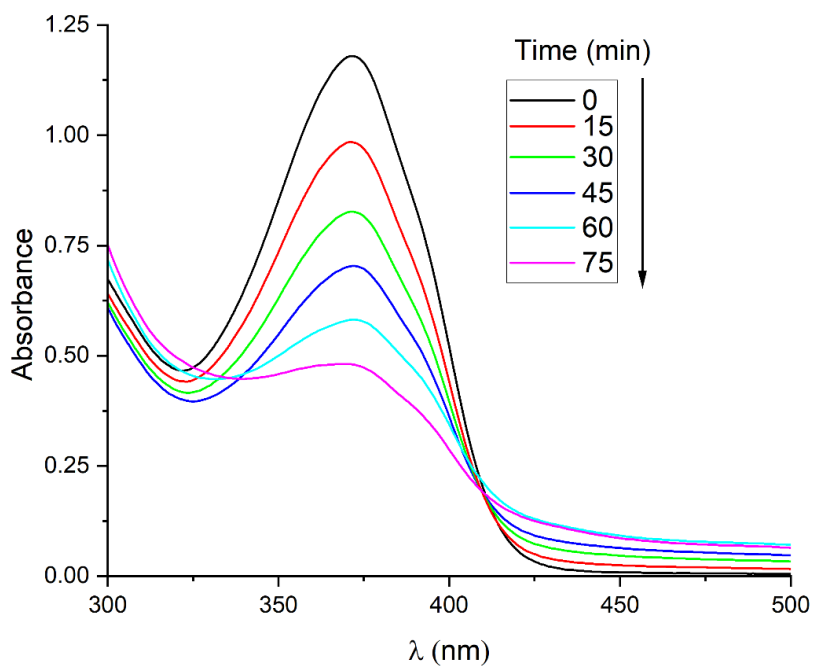


**Fig. S10** Absorption spectra of TC in the presence of SnP-ZnTCPP under visible light irradiation.

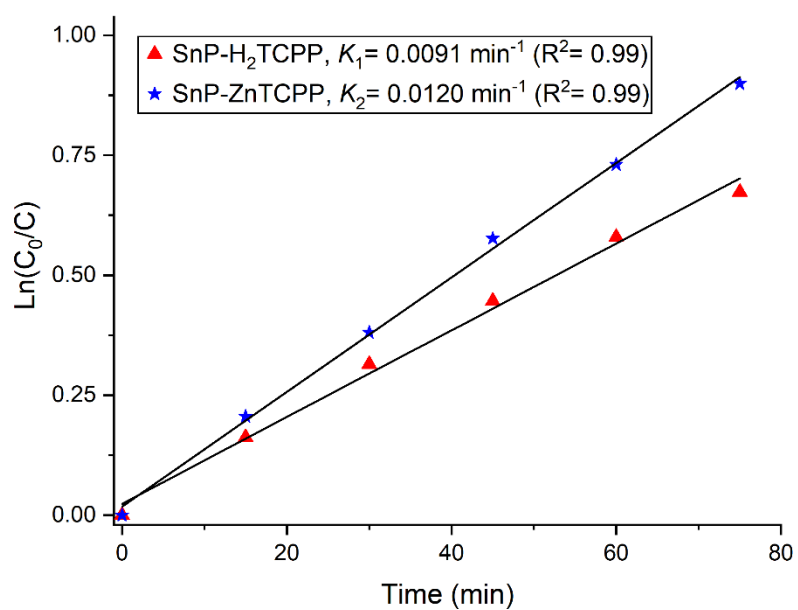


**Fig. S11** Kinetics of the photocatalytic degradation of TC under visible light irradiation.

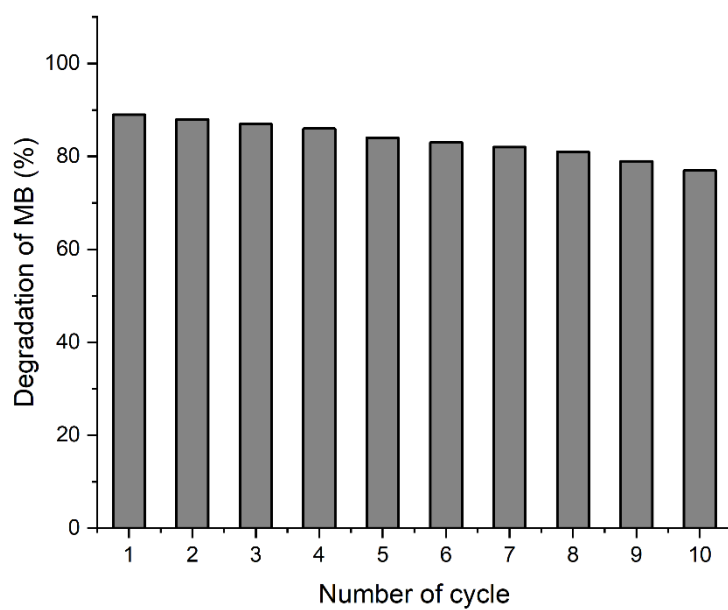


**Fig. S12** Recyclability of the photocatalyst **SnP-H<sub>2</sub>TCPP** towards the degradation of MB dye.

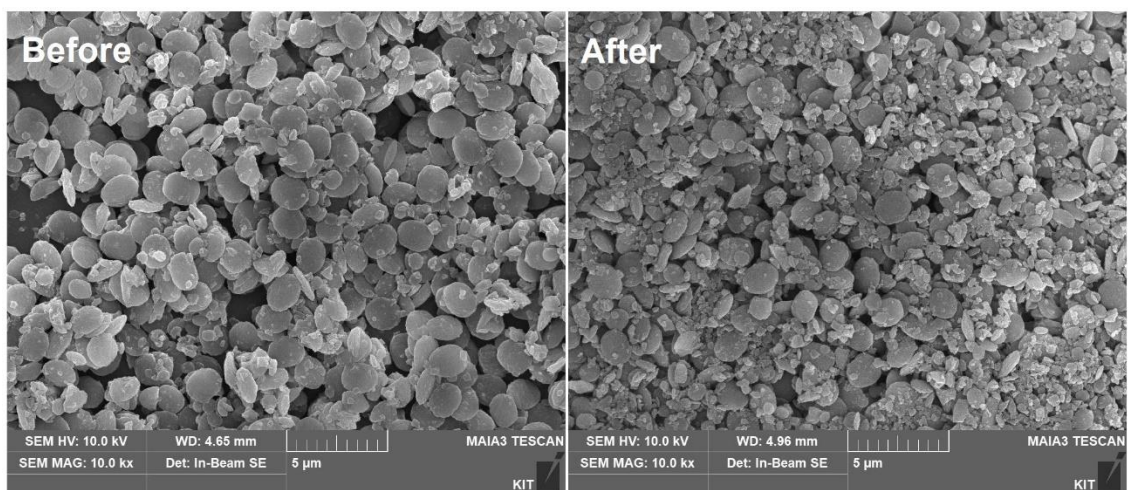


**Fig. S13** FE-SEM images of SnP-H<sub>2</sub>TCPP (before and after the degradation of MB).

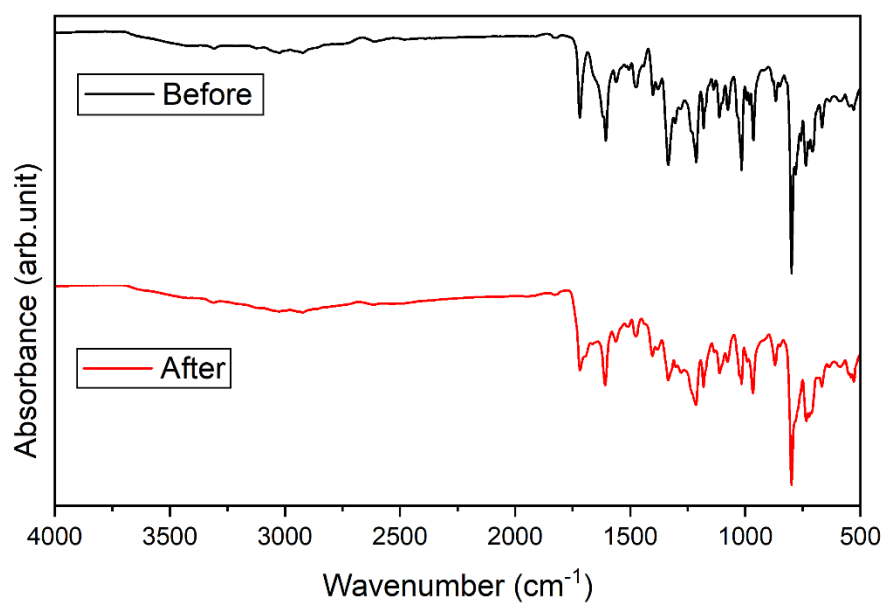


**Fig. S14** FT-IR spectra of SnP-H<sub>2</sub>TCPP (before and after the degradation of MB).

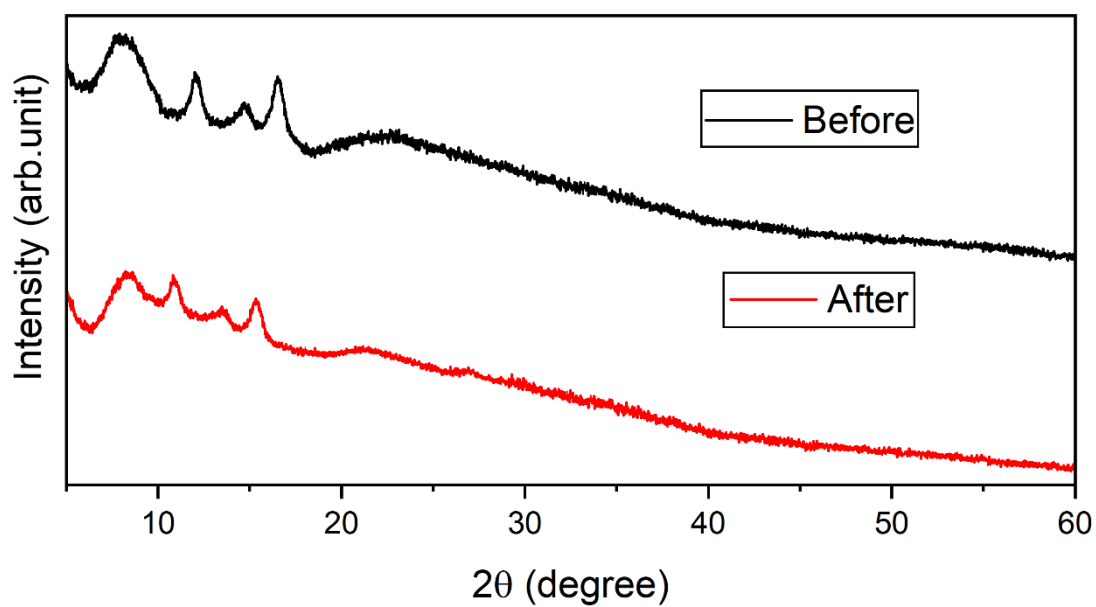


**Fig. S15** PXRD patterns of SnP-H<sub>2</sub>TCPP (before and after the degradation of MB).

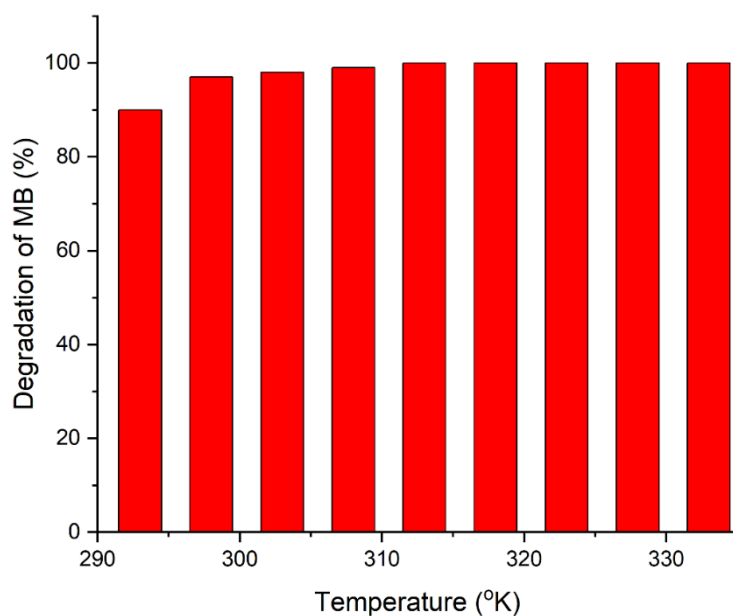


**Fig. S16** Effect of temperature on the photocatalytic degradation of MB dye in the presence of SnP-ZnTCPP.

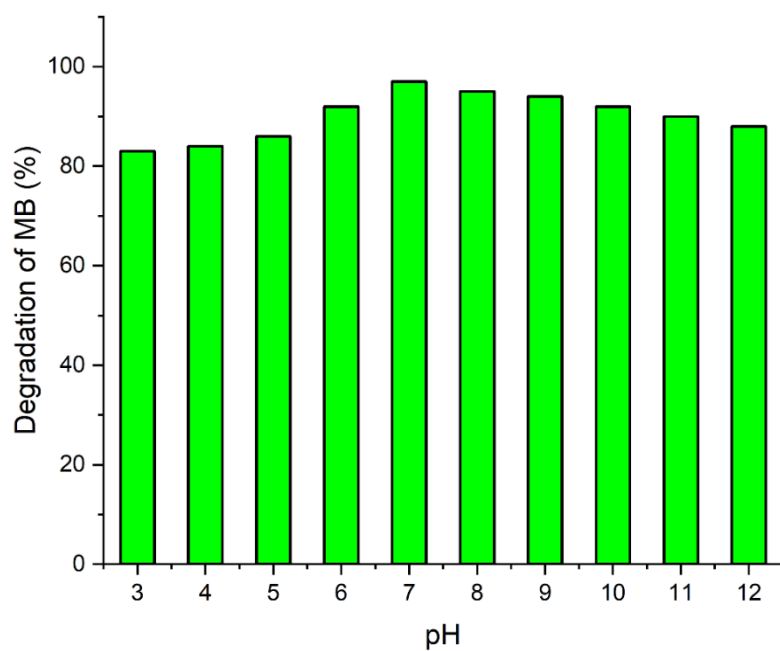


**Fig. S17** Effect of pH on the degradation of MB dye solution in the presence of **SnP-ZnTCPP**.

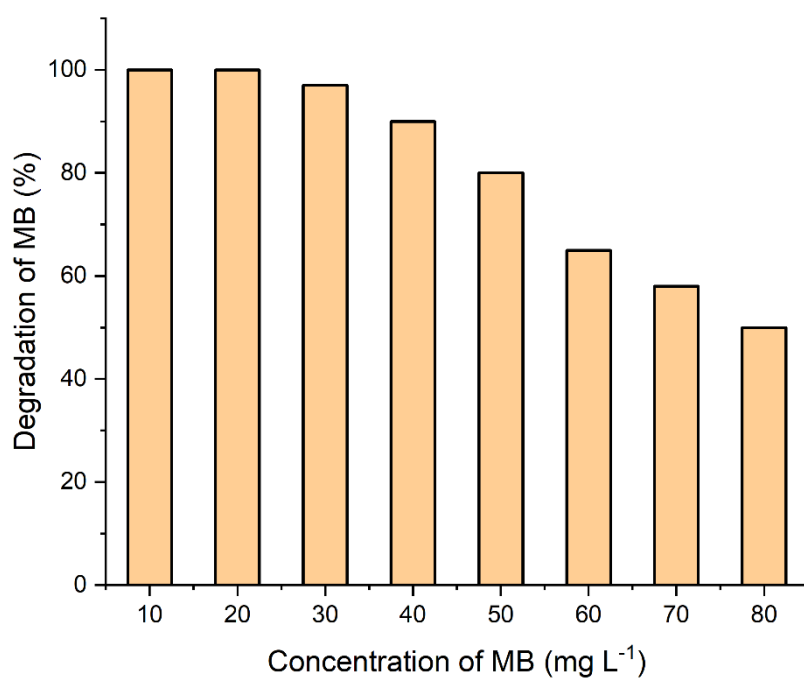


**Fig. S18** Effect of dye concentration on the photocatalytic degradation of MB dye in the presence of **SnP-ZnTCPP**.

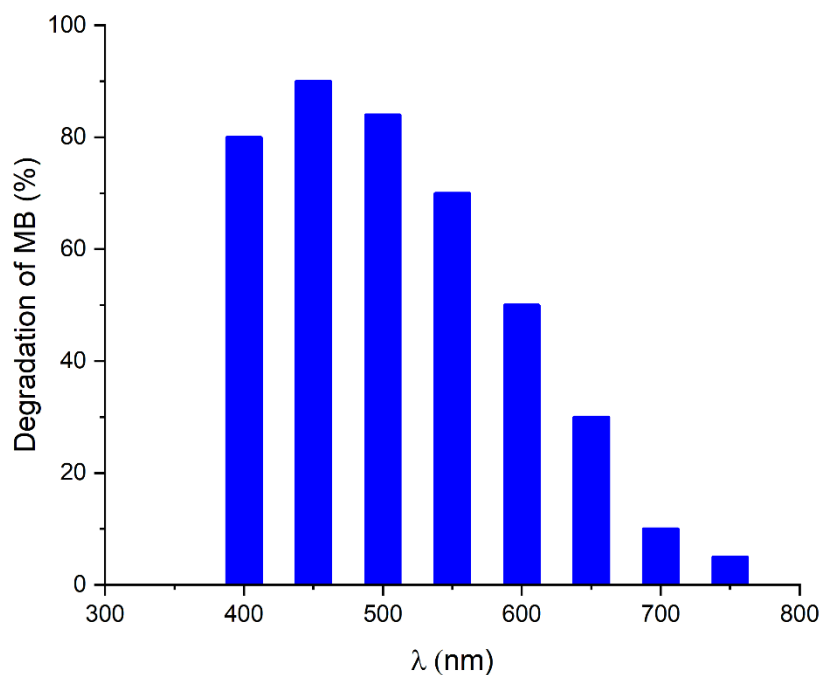


**Fig. S19** Effect of wavelength on the photocatalytic degradation of MB dye in the presence of **SnP-H<sub>2</sub>TCPP**.

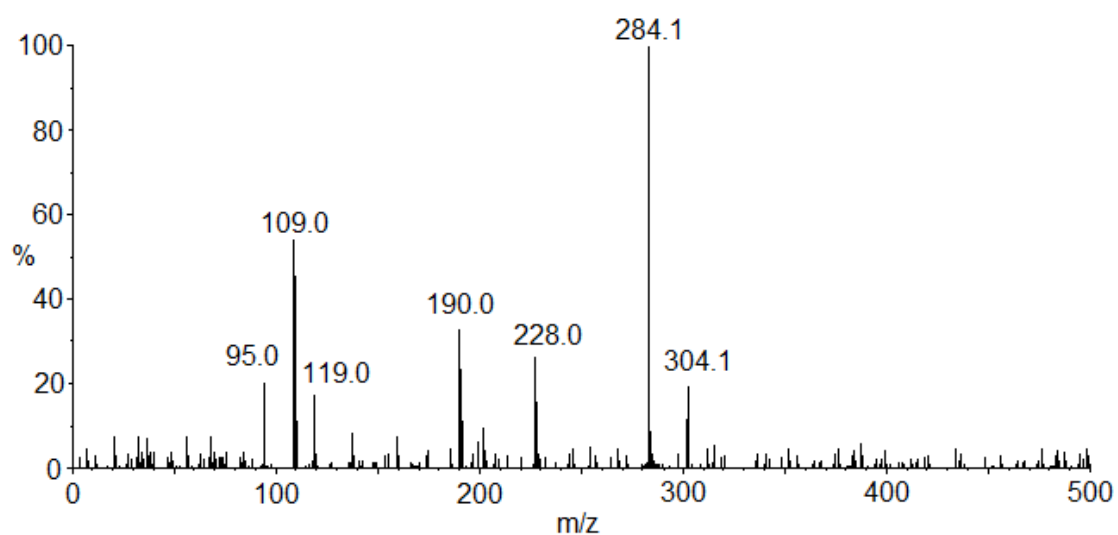


**Fig. S20** Positive ion mode ESI-MS spectrum for the MB dye degradation reaction by **SnP-H<sub>2</sub>TCPP** after 60 min of visible light irradiation.



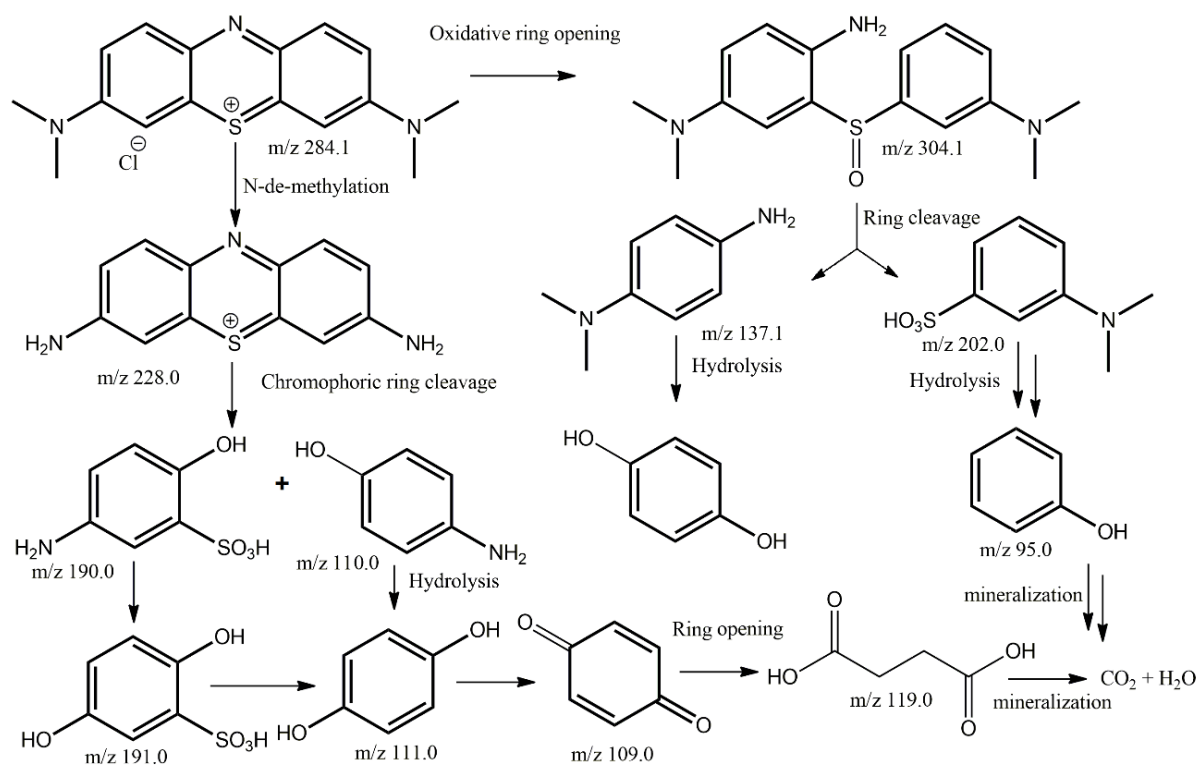


**Fig. S21** Possible intermediates formed during MB dye degradation in the presence of SnP-H<sub>2</sub>TCPP after 60 min of visible light irradiation.

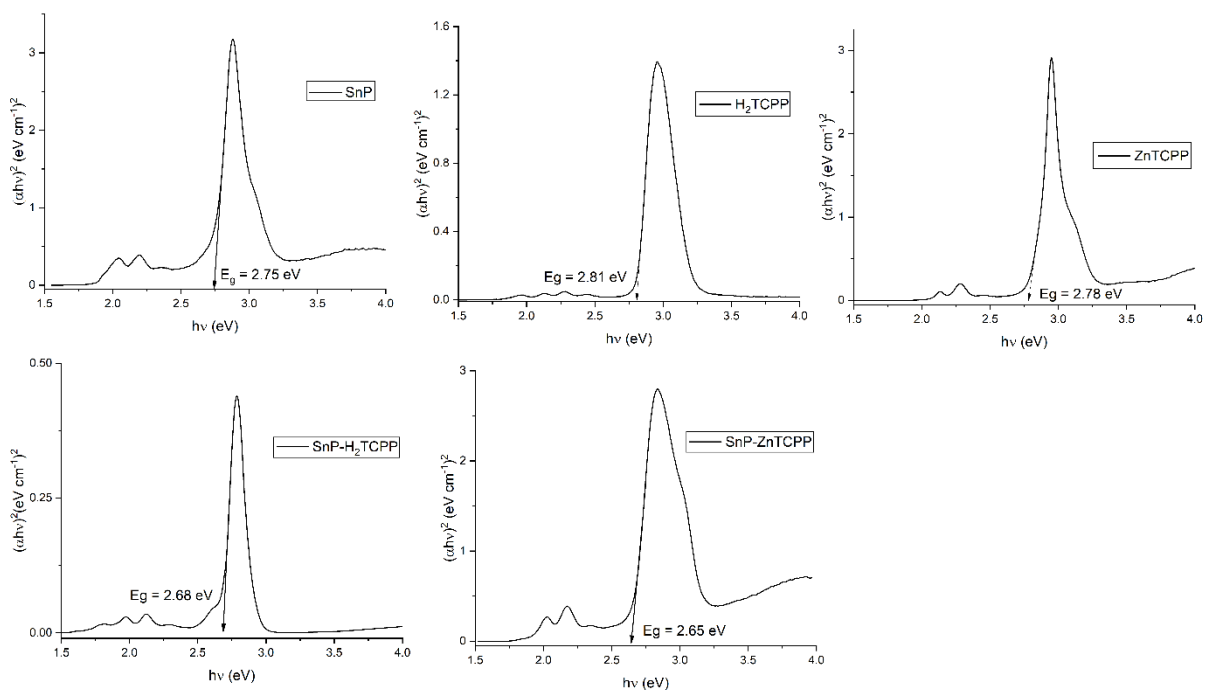


**Fig. S22** Band gap energy of SnP,  $\text{H}_2\text{TCPP}$ , ZnTCPP, SnP- $\text{H}_2\text{TCPP}$ , and SnP-ZnTCPP, calculated from Tauc Plots using UV-vis absorption spectral data.

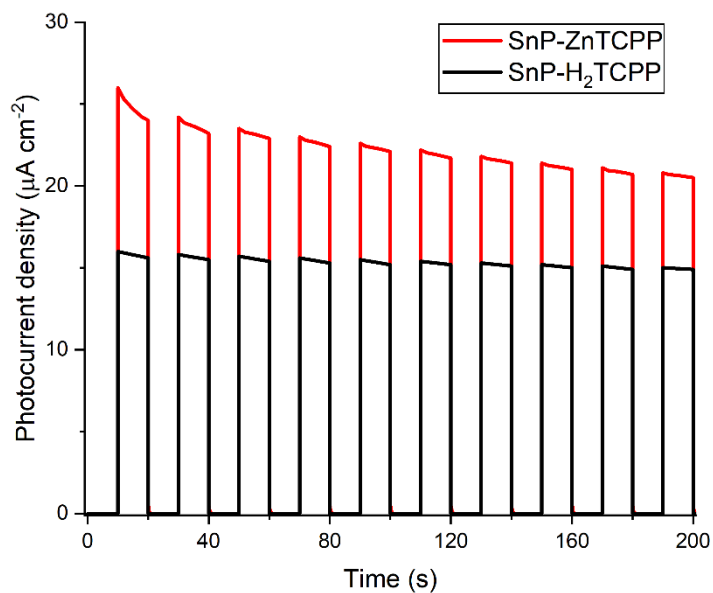


**Fig. S23** Photocurrent responses for SnP- $\text{H}_2\text{TCPP}$  and SnP-ZnTCPP under visible light.

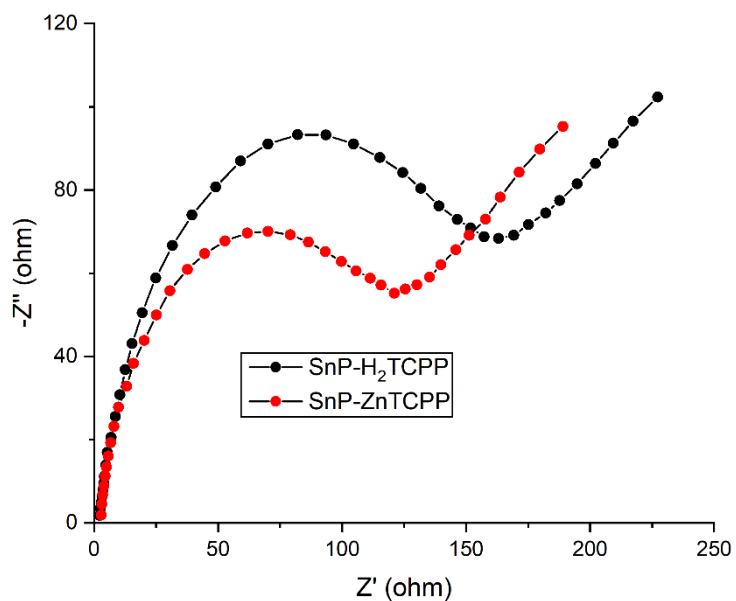


**Fig. S24** EIS Nyquist plots for **SnP-H<sub>2</sub>TCPP** and **SnP-ZnTCPP** under visible light.

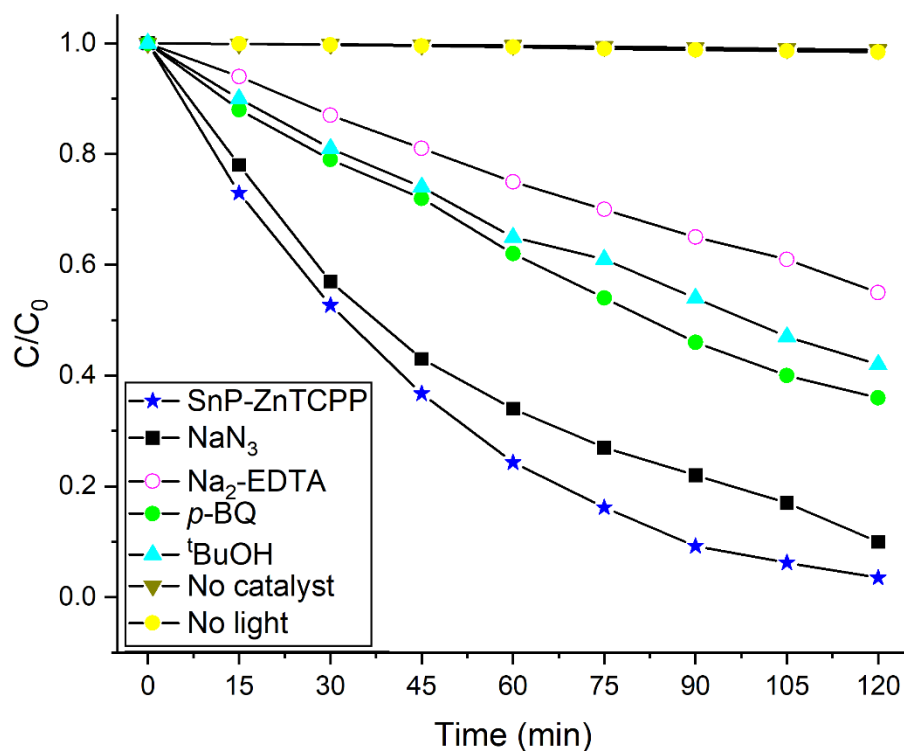


**Fig. S25** Visible light MB dye degradation activity of **SnP-ZnTCPP** in the presence of various scavengers.